Neuron, Volume *78*

Supplemental Information

Associative Learning Enhances Population Coding by Inverting Interneuronal Correlation Patterns

James M. Jeanne, Tatyana O. Sharpee, and Timothy Q. Gentner

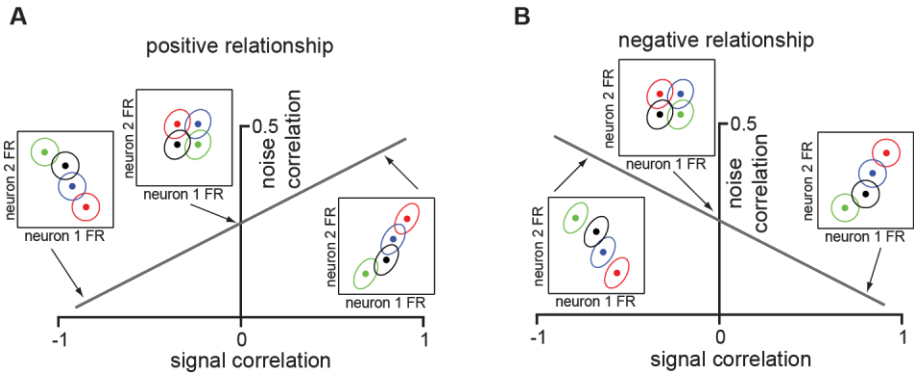

Figure S1, Related to Figure 6. Schematic of relationships between signal and noise correlations.
Each colored dot denotes the mean response for two neurons to each of four stimuli. Each colored ellipse denotes the standard deviation of the two-dimensional response distribution for each stimulus.
(A) For a positive relationship, neuron pairs with positive signal correlation and large noise correlation have substantial overlap in their responses (inset right), while pairs with negative signal correlation and small noise correlation have less overlap (inset left). Center inset depicts pairs with zero signal correlation but moderate noise correlation.
(B) For a negative relationship, neuron pairs with positive signal correlation and small noise correlation have some overlap in their responses (inset right), while neuron pairs with negative signal correlation and large noise correlation have very little overlap (inset left). The negative relationship thus yields neural populations that discriminate between stimuli better than the positive relationship.

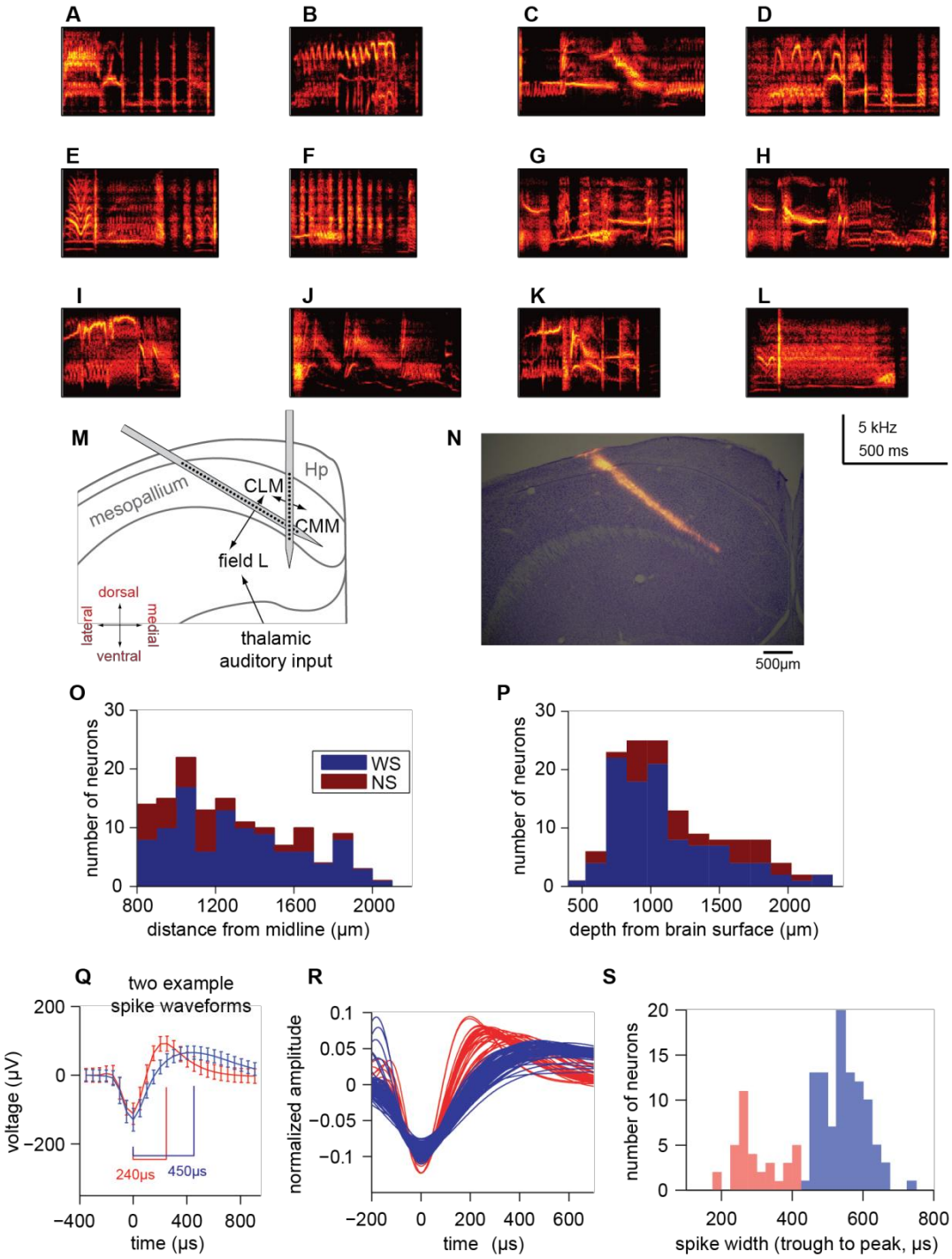

Figure S2, Related to Figure 1. Stimuli, recording setup, and electrophysiology.
(A-L) Spectrograms of motifs used in the study. Each spectrogram is a single motif. During behavioral training, pairs of motifs were concatenated with 20ms of silence between them, as shown in Figure 1C. During neuronal recording, motifs were presented individually.
(M) Schematic showing approximate positioning of multi-channel electrode arrays within CLM. Most data was obtained from 1x32 linear probes inserted at a 35 degree angle. In some birds, a vertical penetration with a 1x16 linear probe was also used.

(N) Nissl stained section showing fluorescent Di-I marking electrode penetration track into CLM. Midline is to the right. Orientation is same as (M).
(O) Distribution of distances from midline within CLM for wide spiking neurons (blue) and narrow spiking neurons (red).
(P) Distribution of depths from the brain surface. Colors are as in (O).
(Q) Spike shapes in CLM. Mean (±S.D.) spike waveforms for a wide (blue) and a narrow (red) spiking neuron (recorded from the same electrode pad) depicting measurement of spike width from trough to peak.
(R) Spike shapes of all neurons recorded in CLM.
(S) Bimodal distribution of spike widths.

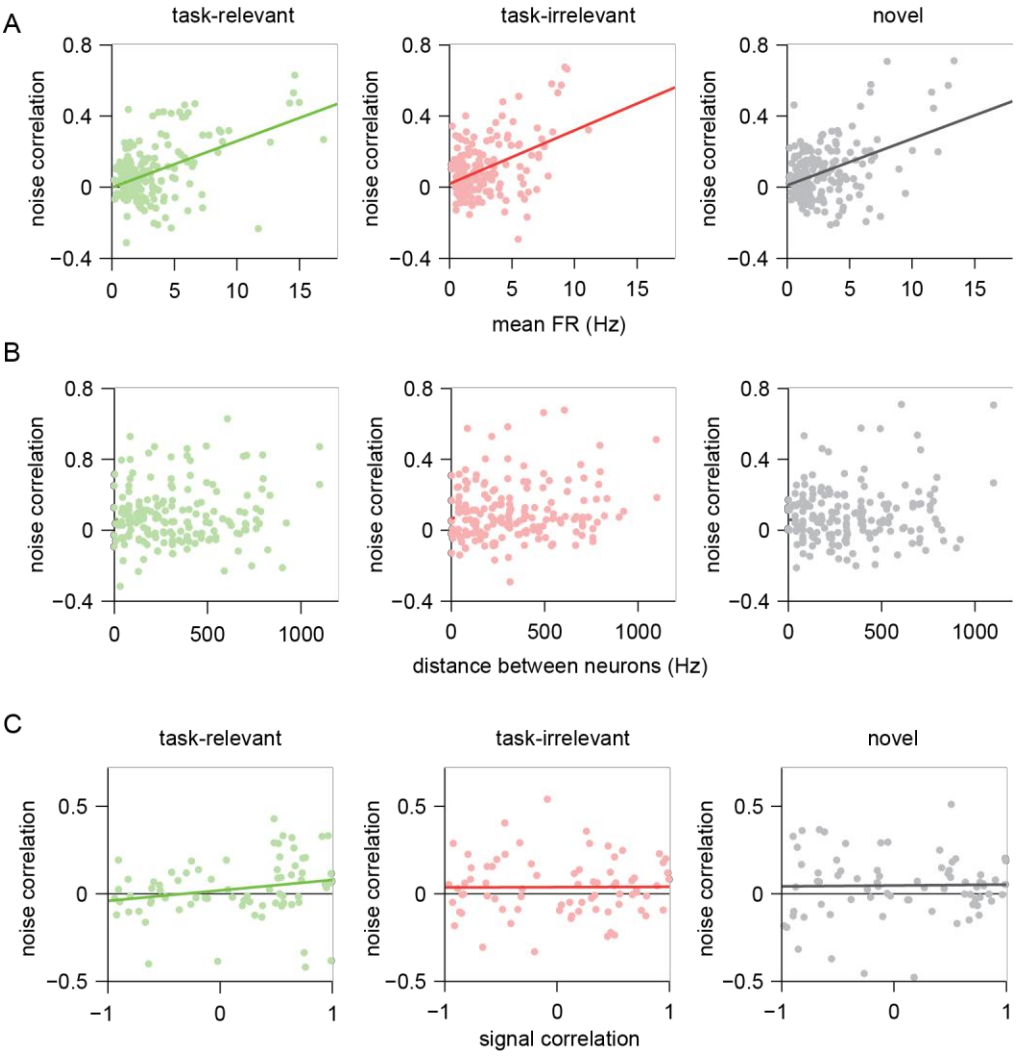

Figure S3, Related to Figure 4. Additional noise correlation comparisons.
(A) Scatter plots of mean firing rate and noise correlation. Noise correlation increases with mean firing rate of the pair, but no difference in this relationship exists between task-relevant (left, green), task-irrelevant (center, red), and novel (right, gray) motifs (ANCOVA motif class × regression slope interaction, $p = 0.77$).
(B) Scatter plots of distance between neurons and noise correlation. No difference in this relationship is observed between task-relevant (left, green), task-irrelevant (center, red), and novel (right, gray) motifs (ANCOVA motif class × regression slope interaction, $p = 0.87$). No statistically significant relationship between distance and noise correlation is observed within any of the three motif classes.
(C) Relationship between signal and noise correlations for NS-NS and NS-WS neuron pairs combined. Signal and noise correlations for task-relevant motifs (left, green), task-irrelevant motifs (center, red), and novel motifs (right, black) ($n = 76$ pairs). Task-relevance did not alter this relationship (ANCOVA motif class × regression slope interaction, $p = 0.38$). Insufficient data were available to analyze NS-NS pairs and NS-WS pairs separately.

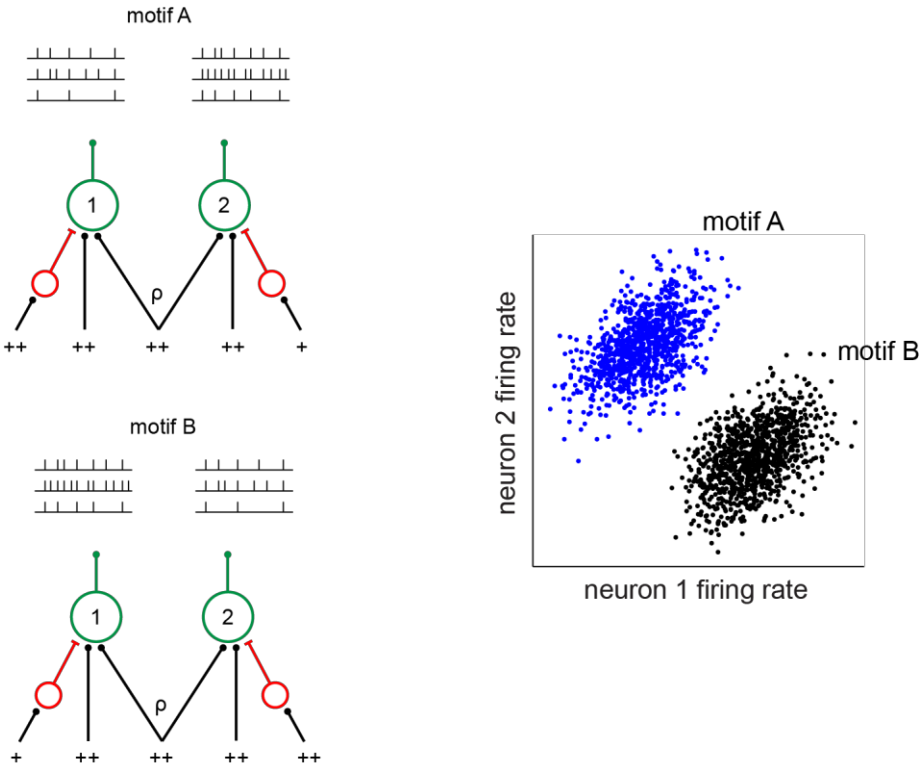

Figure S4, Related to Figure 7. Hypothetical circuit model demonstrating how strong positive noise correlations could coexist with strong negative signal correlations.
Green circles denote excitatory neurons; red circles denote inhibitory neurons. The excitatory neurons (labeled 1 and 2) have both independent input and correlated input. ++ denotes a large magnitude input current and + denotes a small magnitude input current. ρ denotes the fraction of input that is shared. Both excitatory neurons also receive independent feedforward inhibitory input, which is stimulus-dependent. Motif A and motif B drive partially overlapping inputs into these two excitatory neurons. Both motifs drive partially (positively) correlated inputs into neurons 1 and 2, which yields positive noise correlations. However motif A provides independent feedforward inhibition to neuron 1 (but not neuron 2). This suppresses neuron 1's response to motif A, without affecting the noise correlation (as long as neuron 1's response is still positive). Excitatory and inhibitory input need not be perfectly cleanly segregated. Hypothetical spiking output (right panel) shows higher firing rates for neuron 2 than neuron 1, but both neurons exhibit positive trial-by-trial correlations (i.e. noise correaltions). A complementary scenario yields an opposite pattern of mean firing rates for motif B, but maintains the positive noise correlation (bottom left). This circuit could therefore yield the hypothetical set of responses shown at right: positive noise correlation with negative signal correlation.

Supplemental Experimental Procedures

Electrophysiology

Approximately 24 hours prior to electrophysiological recording, the animal was anesthetized (1.5-2% isoflurane), a small pin was attached to the surface of the skull just caudal to CLM, and the animal was allowed to recover. On the recording day, starlings were anesthetized with urethane (20% by volume, 7-8ml/kg) and head-fixed via the attached pin to a stereotactic apparatus inside a sound-attenuating chamber. A small craniotomy was made dorsal to CLM, and multi-channel silicon electrode arrays (177µm2 electrode surface area, 50µm spacing, 1x16 and 1x32 electrode layout; NeuroNexus technologies). 1x32 electrode arrays were generally inserted at a 35° angle (relative to horizontal) and simultaneously measured neural activity across the medial-lateral axis of CLM. 1x16 electrode arrays were generally inserted at a 90° angle (relative to horizontal). For some subjects, only the 1x32 array was used (Supplemental Figure S2M). Motif stimuli were presented free field from a speaker 30cm from the bird at sound pressure levels matched to those during behavioral training (mean, 65dB; peak, 96dB). Electrode arrays were advanced while presenting the 12 motif stimuli until 2 or more auditory single units were isolated. Once single units were isolated, all 12 single motifs and the set of training motif pairs were presented pseudo-randomly in blocks while the extracellular electrical activity was amplified (5000× gain; AM Systems), filtered (high pass, 300Hz; low pass, 3-5kHz), sampled (20kHz), and saved digitally for offline analysis (Spike2; Cambridge Electronic Design). Electrodes were coated with Di-I to facilitate localization of penetration tracks in histological sections.

Histology

At the end of the recording session, starlings were euthanized with an overdose of nembutal (150ml/kg), and perfused transcardially with 10% neutral buffered formalin. Brains were removed from the skull and placed in 30% sucrose solution for several days for cryoprotection. Brains were then cut into 50µm coronal sections on a freezing microtome and mounted on glass slides. Electrode penetration tracks were identified with the assistance of Di-I marking and epifluorescence microscopy (Supplemental Figure S2N). Tissue was then stained with cresyl violet to localize penetration tracks to neuroanatomical boundaries. All electrode tracks were reconstructed from tissue sections, and the recording locations of all sites were measured. The medial boundary of CLM was taken to be 800µm from the midline. Recording locations for CLM neurons ranged from 810-2100µm from the midline, and from 507-2240µm from the dorsal surface (Supplemental Figure S2O,P).